Usefulness of Prebiopsy Multifunctional and Morphologic MRI Combined With Free-to-Total Prostate-Specific Antigen Ratio in the Detection of Prostate Cancer

Joan C. Vilanova[1,2,3]
Carles Barceló-Vidal[4]
Josep Comet[5]
Maria Boada[1]
Joaquim Barceló[1,2,3]
Joana Ferrer[3]
Joan Albanell[3]

OBJECTIVE. The purpose of the study was to assess the predictive value for prostate cancer of MRI using morphologic (T2-weighted imaging [T2WI]) and functional (MR spectroscopy [MRS], diffusion-weighted imaging [DWI], and dynamic contrast-enhanced [DCE] MRI) sequences and the free-to-total prostate-specific antigen (PSA) ratio, alone and combined.

MATERIALS AND METHODS. This retrospective study included 70 patients (PSA level, > 4 ng/mL; free-to-total PSA ratio, < 20%) who underwent endorectal 1.5-T MRI before biopsy. We graded the likelihood of cancer on a 5-point scale. Imaging data were compared with histologic results on biopsy or prostatectomy. Accuracies were estimated from the area under receiver operating characteristic using the hemiprostate as the unit of analysis. A *p* value less than 0.05 denoted statistical significance.

RESULTS. The model combining all variables was more accurate than each variable alone (95.2% vs 73.5% for T2WI, 76.0% for MRS, 81.8% for DWI, 75.6% for DCE-MRI, and 78.8% for free-to-total PSA ratio). The complete model had accuracy similar to that of combining two imaging variables with free-to-total PSA ratio, especially free-to-total PSA ratio, T2WI, and DWI (94.0%); and free-to-total PSA ratio, DWI, and MRS (93.8%); with negative predictive values of 91.0% and 89.5%, respectively. The best models combining two imaging variables (MRS and DWI, 85.8%; T2WI and DWI, 84.8%) had accuracy that was similar to that of the combination of all imaging variables (87.3%) and higher than that of the best individual imaging variable (DWI, 81.8%), but lower than that of the complete model.

CONCLUSION. The combination of at least one functional technique with free-to-total PSA ratio is more accurate than combining only imaging variables in cancer detection. The use of more than two imaging variables does not increase the detection rate. Functional MRI has the potential to help avoid a large number of negative biopsies.

Keywords: contrast-enhanced MRI, diffusion, MRI, prostate, spectroscopy

DOI:10.2214/AJR.10.5700

Received September 2, 2010; accepted after revision November 3, 2010.

This work was supported by the Spanish Radiologic Society (grant SERAM07JCVB 06), the Spanish Ministry of Science (grant MTM2009-13272), and the Agència de Gestió d'Ajuts Universitaris i de Recerca of the Generalitat de Catalunya (grant 2009SGR424).

[1]Department of MRI, Clínica Girona, Lorenzana 36, Girona 17002, Spain. Address correspondence to J. C. Vilanova (kvilanova@comg.cat).

[2]Department of Medical Science, Faculty of Medicine, University of Girona, Girona, Spain.

[3]Department of Radiology, Hospital St. Caterina, Girona, Spain.

[4]Department of Computer Science and Applied Mathematics, University of Girona, Campus Montilivi, Girona, Spain.

[5]Department of Urology, Hospital Dr. J. Trueta, Girona, Spain.

WEB
This is a Web exclusive article.

AJR 2011; 196:W715–W722

0361–803X/11/1966–W715

Prostate cancer is the most common noncutaneous malignancy among men in the developed world and represents an important health care burden. The most common diagnostic methods to detect prostate cancer are digital rectal examination (DRE) and serum prostate-specific antigen (PSA) levels. The accuracy of both methods is suboptimal. In particular, the specificity of PSA is very low: 70–80% of patients with the usual clinical cutoff level (PSA > 4 ng/mL) do not have prostate cancer [1, 2]. Consequently, 60–75% of men with PSA levels greater than 4 ng/mL undergo unnecessary biopsy. Moreover, elevated PSA levels and multiple negative transrectal ultrasound (TRUS)–guided biopsies cannot entirely rule out cancer [3]. Over the past decade, standard MRI combined with functional imaging techniques, such as MR spectroscopy (MRS), diffusion-weighted imaging (DWI), or dynamic contrast-enhanced (DCE) MRI, have shown promising results for prostate cancer detection [4–15]. Furthermore, including MRI or MRS in the diagnostic workup of patients with elevated PSA level and low free-to-total PSA ratio or PSA density may be useful to select patients at risk and improve the detection of prostate cancer before TRUS-guided biopsy [16, 17].

We aimed to assess the value of endorectal MRI combined with functional MRI (MRS, DWI, or DCE-MRI) and the free-to-total PSA ratio for detecting prostate cancer before the biopsy in men with elevated PSA levels and to determine which functional parameter or combination of parameters is most useful for prostate cancer detection.

Materials and Methods

Patients and Study Design

We identified retrospectively all patients who were referred for endorectal MRI between May 2008 and September 2009 who met the following inclusion criteria: no previous prostate biopsy, PSA levels greater than 4 ng/mL, and free-to-total PSA ratio less than 20%. Our institutional review board approved this study, and informed consent was obtained from all patients. Exclusion criteria were prior biopsy, poor general health contraindicating biopsy or prostatectomy or both, previous diagnosis of acute prostatitis, history of prostate cancer, and contraindications to MRI (e.g., cardiac pacemakers and intracranial clips) or to endorectal coil insertion (e.g., anorectal surgery or inflammatory bowel disease).

Our primary selection included 78 patients, of whom eight were excluded, five because pathologic data were unavailable and three because images were distorted. Blood samples for PSA levels and free-to-total PSA ratio were obtained before DRE and always were processed at the same laboratory.

The final study population consisted of 70 men (PSA levels, 4–17.20 ng/mL [median, 7.4 ng/mL]; free-to-total PSA ratio, < 20%) with a mean age of 63.5 years (range, 43–87 years). The median Gleason score was 7 (range, 5–8). The time interval between MRI examination and biopsy was 13 ± 9 days.

MRI Technique

MRI studies were performed with a 1.5-T whole-body MRI unit (Signa Horizon HDx, GE Healthcare). A body coil was used for excitation, and a pelvic four-channel phased-array coil in combination with a commercially available balloon-covered expandable endorectal coil (Endo ATD, Medrad) was used for signal reception. The endorectal coil was positioned with the patient in recumbent lateral position insufflating with 80–100 mL of air.

Transverse T1-weighted sequences with the following parameters were acquired: TR/TE, 500/12; section thickness, 5 mm; intersection gap, 1 mm; field of view, 24 cm; matrix, 256 × 192; transverse frequency encoding; one excitation; and acquisition time, 5 minutes 53 seconds of the pelvic region from the aortic bifurcation to the symphysis pubis. Transverse and coronal high resolution fast spin-echo T2WI of the prostate and seminal vesicles was performed with the following parameters: 5000/102; echo-train length, 16; section thickness, 3 mm; intersection gap, 0 mm; field of view, 14 cm; matrix, 256 × 192; anteroposterior frequency encoding; three excitations; and acquisition time, 3 minutes 22 seconds.

MRS data were acquired within a volume around the prostate after reviewing the transverse T2WI scans. A box was positioned on transverse T2WI scans to include the prostate gland. Three-dimensional MRS data were acquired using a water- and lipid-suppressed double spin-echo point-resolved spectroscopy sequence optimized for the quantitative detection of choline and citrate. To achieve the water and lipid suppression, a band-selective inversion with gradient dephasing technique was used. No examinations were discarded because of inadequate magnetic field homogeneity. The 3D MRS dataset was acquired with a spatial resolution of 0.24–0.34 cm^3, 1000/130 milliseconds as 16 × 8 × 8 phase-encoded spectral arrays (1024 voxels), and 19-minute acquisition time. The 3D MRS data were processed and aligned with the corresponding MRI scan on a workstation using specific commercial software for analyzing 3D MRS studies (Functool, GE Healthcare). Peak areas for choline, creatine, and citrate were calculated using numeric integration. Metabolic ratio maps of the ratio of choline plus creatine to citrate were generated. Signal-to-noise ratio values were automatically calculated as the ratio between citrate or choline peak amplitude and the SD of the noise over the 0.40–0.96 ppm range. Voxels were considered suitable if they consisted of at least 75% peripheral zone tissue, did not include periurethral tissue or ejaculatory ducts, had signal-to-noise ratio of greater than 5:1, and were not spectroscopically contaminated by insufficient water or fat suppression.

DWI was performed using a single-shot echo-planar imaging technique with the following parameters: 8250/94; field of view, 26 cm; section thickness, 3 mm; intersection gap, 0 mm; matrix, 128 × 128; number of excitations, 6; acquisition time, 1 minute 23 seconds; and b values, 0 and 1.000 s/mm^2.

DCE-MRI was obtained using a multisection T1-weighted 3D spoiled gradient-echo sequence (14/1.8; flip angle, 12°; sections, 30; section thickness, 4 mm; no intersection gap; field of view, 260 mm; matrix, 160 × 256; and temporal resolution, 6 seconds) in the axial plane before and 30 times during IV bolus injection, without delay, of gadopentetate dimeglumine (Magnevist, Bayer Schering Pharma) at a dose of 0.1 mmol/kg through a peripheral vein at a rate of 3 mL/s.

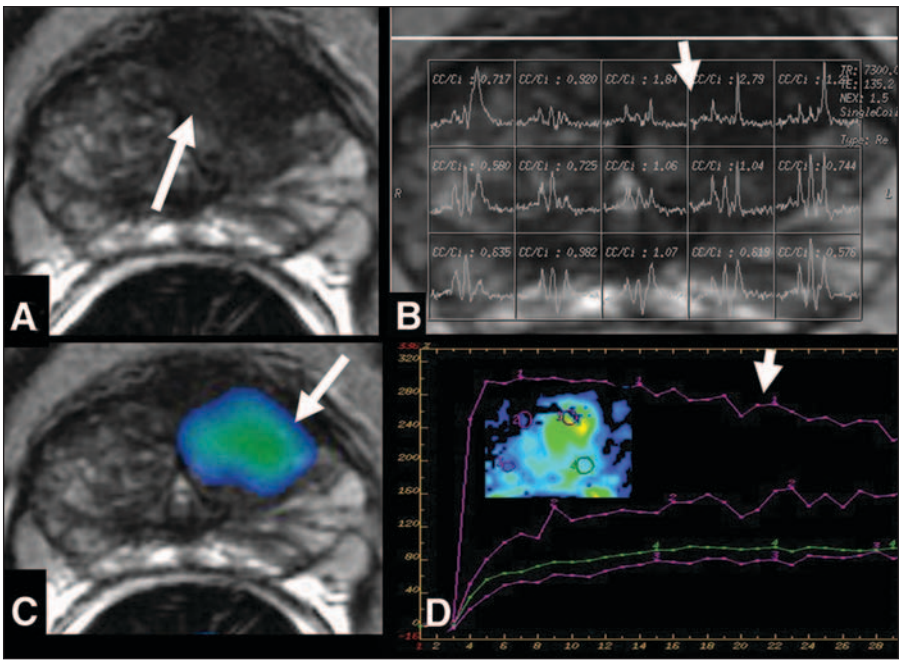

Fig. 1—70-year-old man with transitional prostate cancer, with positive MRI results on T2-weighted imaging (T2WI), MR spectroscopy (MRS), diffusion-weighted imaging (DWI), and dynamic contrast-enhanced (DCE) MRI images. Patient's prostate-specific antigen (PSA) level was 7.60 ng/mL, and his free-to-total PSA ratio was 14.5%.
A, Axial T2WI scan shows low-signal-intensity nodular ill-defined lesion (*arrow*) within left transitional zone suspicious for cancer.
B, MRS image shows pathologic metabolic curve within voxels from lesion (*arrow*).
C, Apparent diffusion coefficient color map from DWI combined with T2WI shows restricted diffusion from lesion (*arrow*), suspicious for malignant tumor.
D, DCE-MRI image on color-coded graph shows curve type 3 from region of interest (ROI) of lesion (*arrow*) suspicious for cancer, whereas other ROIs show type 1 curve. Biopsy was positive for prostate cancer within transitional zone.

Image Interpretation

Three radiologists; with 14, 8, and 6 years experience in prostate MRI interpretation, respectively, evaluated in consensus all the MRI, MRS, DWI, and DCE-MRI scans while blind to clinical findings. For tumor localization, the prostate was split along the midline and further divided into the apex, middle, and base of the peripheral zone; and the transitional left and right zone. Thus, in each case, the prostate was divided into eight regions. The imaging evaluation consisted of four parts: First, the three readers interpreted and scored the T2WI scans using a 5-point scale. The presence of cancer on T2WI, identified as an area of low signal intensity within the peripheral and transitional zone [18], was recorded for each region on a standardized form developed for this study. Readers graded their confidence that cancer was present in each region on a 5-point scale, as follows: 1, definitely no tumor; 2, probably no tumor; 3, tumor possible; 4, tumor probable; and 5, tumor definitely present.

Second, all MRS data were read after the first MRI datasets. All readers randomly interpreted the MRI and MRS datasets independently.

All the voxels within each of the six regions of the prostate were judged, and each region was scored on the 5-point scale described previously in the article as a function of mean values of the ratio of choline plus creatine to citrate calculated from the mean ratio previously published for healthy prostate tissue in the peripheral zone [19] as follows: 1, ratio of less than 0.5; 2, ratio of 0.5 or less than 0.6; 3, ratio of 0.6 or less than 0.7; 4, ratio of 0.7 to less than 0.8; and 5, ratio of 0.8 or greater. For the transitional zone, scores were assigned as follows: 1, ratio of less than 0.8; 2, ratio of 0.8 to less than 0.9; 3, ratio of 0.9 or less than 1.0; 4, ratio 1.0; and 5, ratio of 1.1 or greater.

Third, apparent diffusion coefficient (ADC) values were obtained from the DWI sequence from each of the eight regions. Several 5-mm^2 regions of interest (ROIs) were placed in each region, and the minimum ADC value was selected from each region. The ADC values were categorized on a 5-point scale as follows [8]: 1, ADC value of 1.6×10^3 mm^2/s or higher; 2, ADC values of 1.4 or less than 1.6×10^3 mm^2/s; 3, ADC values of 1.2 or less than 1.4×10^3 mm^2/s; 4, ADC values of 1.0 or less than 1.2×10^3 mm^2/s; and 5, ADC values less than 1.0×10^3 mm^2/s.

Fourth, DCE-MRI parameters were evaluated on a dedicated workstation with commercial software (CADstream, Merge) to fit curves for analysis. The most suspicious curve from each region was obtained after placing several ROIs of 5 mm^2 on each region. Curves were classified into three types, as follows [20]: type 1, persistent enhancement and no suspicious criteria; type 2, early fast enhancement followed by a plateau phase in which signal intensity remained constant within the acquisition with no more than 10% change from the peak enhancement and with moderate suspicious criteria; or type 3, early fast enhancement followed by washout (greater than 10% decrease in signal intensity after the peak enhancement) and high suspicious criteria. DCE-MRI regions were categorized on the 5-point scale described previously as follows: 1, regions with no enhancement or a symmetric or asymmetric type 1 curve; 2, regions with a symmetric type 2 curve; 3, regions with an asymmetric type 2 curve; 4, regions with a symmetric type 3 curve; and 5, regions with an asymmetric type 3 curve.

Biopsy

After standard preparation, all patients underwent TRUS-guided biopsy with an ultrasound scanner with a 6.5-MHz sector probe (Allegra, Siemens Healthcare). Eight prostatic cores were obtained using an 18-gauge biopsy needle (Tru-Cut, Bard Urologic) with a spring-loaded biopsy gun (Manan Medical). At least two cores were obtained from each of the six regions of the peripheral gland, and two additional cores were obtained from the transitional zone on each side of the gland. Additional biopsies were targeted by the same operator toward areas with features that raised the suspicion of tumor by ultrasound. All cores were labeled according to their octant topographic location as the base, midgland, apex, or transitional zone from each side of the gland. All biopsies were performed by one radiologist who was unaware of the clinical and imaging findings.

Standard of Reference

The material for histopathologic analysis was the biopsy core in 57 patients and the prostatic gland after prostatectomy in 13 patients. The histopathologic analysis included determination of the number of cores positive for prostate cancer. The biopsy cores and surgical specimens were analyzed according to the schematic diagram described previously, in which the prostate is divided into eight regions. Aligning the imaging data and histopathologic evaluation is considered difficult [7].

Statistical Analysis

Because of the known limitations of tumor localization of the precise octant [21] when using biopsy, we used the hemiprostate (i.e., left and right sides of the gland) as the unit of statistical analysis for T2WI, MRS, DWI, and DCE-MRI. Thus, we took for each predictive variable the maximum value of the four readings on the left hemiprostate and the maximum value of the four readings on the right hemiprostate. Cancer was determined to be present or absent in each hemiprostate on the basis of the presence or absence of an ipsilateral positive biopsy or prostatectomy result.

We first separately evaluated the diagnostic accuracy of each of the five predictive variables T2WI (5-point ordinal scale), MRS (5-point ordinal scale), DWI (5-point ordinal scale), DCE-MRI (5-point ordinal scale), and free-to-total PSA ratio (continuous scale) by fitting generalized estimated equation (GEE) logistic regression models with those variables as numeric predictor variables. We used the statistical approach based on the GEE method because the two hemiprostate readings of the same patient were correlated. It was necessary to introduce a working correlation matrix into the generalized linear model. The correlation structure used in the predictive logistic models was exchangeable. The results did not support linearity in the logit for any of those predictive variables. Therefore, we decided to dichotomize the scores: the ordinal variables T2WI, MRS, DWI, and DCE-MRI were dichotomized by assigning 0 to scores of 1–2, and 1 to scores of 3–5; free-to-total PSA ratio was dichotomized by assigning 1 to the range 0–15% and 0 to the range greater than 15% [22]. Then we analyzed the predictive accuracy of the dichotomized variables for the diagnosis of prostate cancer both individually and considering all possible combinations among them. Accuracies were estimated from the area under receiver operating characteristic (ROC) curves (AUC) drawn from the estimated probabilities given by the corresponding logistic regression models. We compared the accuracy of any two predictive models by comparing the AUCs of the corresponding ROC curves using the DeLong, DeLong, Clarke-Pearson algorithm [23]. We also calculated the sensitivity, specificity, positive predictive value (PPV), and negative predictive value (NPV) of each model taking, from the associated ROC curve, the optimal cutoff value corresponding to maximal Youden index. The sensitivities and specificities of any two predictive models were compared using the exact McNemar test. To compare PPVs and NPVs, we used the GEE method, as described elsewhere [24]. For each model, sensitivity, specificity, PPV, and NPV on a per-patient basis for cancer detection were also calculated from the predictions given by the model in the two hemiprostates of each patient.

All p values less than 0.05 were considered statistically significant. Statistical analyses were performed using statistical software (Stata version 9.0, StataCorp).

Results

Histopathologic analysis detected prostate cancer in 54.2% (38/70) of patients. Cancer was bilateral in 18.6% (13/70) of patients and unilateral in 35.7% (25/70) of patients.

TABLE 1: Estimated Accuracy (Area Under Receiver Operating Characteristic Curve), Sensitivity, Specificity, Positive Predictive Value (PPV), and Negative Predictive Value (NPV) of Dichotomized Variables and Some Combinations of These Variables for Detection of Hemiprostate Cancer

Combinations of Variables	Accuracy (%)[a]	Sensitivity (%)	Specificity (%)	PPV (%)	NPV (%)
Individual variables					
DWI	81.8	72.5	91.0	82.2	85.3
Free-to-total PSA ratio	78.8 (0.513)	98.0	59.6	58.1	98.2
MRS	76.0 (0.159)	66.7	85.4	72.3	81.7
DCE-MRI	75.6 (0.100)	72.5	78.7	66.1	83.3
T2WI	73.5 (0.039)	78.4	68.5	58.8	84.7
Two imaging variables					
MRS plus DWI	85.8	72.5	91.0	82.2	85.3
T2WI plus DWI	84.8 (0.688)	72.5	91.0	82.2	85.3
DWI plus DCE-MRI	84.6 (0.566)	72.5	91.0	82.2	85.3
T2WI plus MRS	81.4 (0.122)	86.3	66.3	59.5	89.4
MRS plus DCE-MRI	81.0 (0.075)	82.4	75.3	65.6	88.2
T2WI plus DCE-MRI	80.0 (0.077)	72.5	78.7	66.1	83.3
Three imaging variables					
T2WI plus MRS plus DWI	87.4	72.5	91.0	82.2	85.3
MRS plus DWI plus DCE-MRI	86.6 (0.551)	72.5	91.0	82.2	85.3
T2WI plus DWI plus DCE-MRI	85.9 (0.298)	72.5	91.0	82.2	85.3
T2WI plus MRS plus DCE-MRI	83.3 (0.023)	82.4	75.3	65.6	88.2
All imaging variables, T2WI plus MRS plus DWI plus DCE-MRI	87.3	72.5	91.0	82.2	85.3
All imaging models					
T2WI plus MRS plus DWI plus DCE-MRI	87.3	72.5	91.0	82.2	85.3
T2WI plus MRS plus DWI	87.4 (0.873)	72.5	91.0	82.2	85.3
MRS plus DWI plus DCE-MRI	86.6 (0.557)	72.5	91.0	82.2	85.3
T2WI plus DWI plus DCE-MRI	85.9 (0.177)	72.5	91.0	82.2	85.3
T2WI plus MRS plus DCE-MRI	83.3 (0.011)	82.4	75.3	65.6	88.2
MRS plus DWI	85.8 (0.375)	72.5	91.0	82.2	85.3
T2WI plus DWI	84.8 (0.110)	72.5	91.0	82.2	85.3
DWI plus DCE-MRI	84.6 (0.087)	72.5	91.0	82.2	85.3
T2WI plus MRS	81.4 (0.015)	86.3	66.3	59.5	89.4
MRS plus DCE-MRI	81.0 (0.007)	82.4	75.3	65.6	88.2
T2WI plus DCE-MRI	80.0 (< 0.001)	72.5	78.7	66.1	83.3
DWI	81.8 (0.014)	72.5	91.0	82.2	85.3
MRS	76.0 (< 0.001)	66.7	85.4	72.3	81.7
DCE	75.6 (< 0.001)	72.5	78.7	66.1	83.3
T2WI	73.5 (< 0.001)	78.4	68.5	58.8	84.7
All imaging models plus free-to-total PSA ratio					
T2WI plus MRS plus DWI plus DCE-MRI plus free-to-total PSA ratio	95.2	88.2	89.9	83.3	93.0
T2WI plus MRS plus DWI plus free-to-total PSA ratio	95.2 (0.951)	88.2	91.0	84.9	93.1
MRS plus DWI plus DCE-MRI plus free-to-total PSA ratio	94.6 (0.307)	86.3	89.9	83.0	92.1
T2WI plus DWI plus DCE-MRI plus free-to-total PSA ratio	94.3 (0.292)	86.3	89.9	83.0	92.1
T2WI plus MRS plus DCE-MRI plus free-to-total PSA ratio	94.1 (0.243)	88.2	89.9	83.3	93.0
MRS plus DWI plus free-to-total PSA ratio	93.8 (0.156)	80.4	95.5	91.1	89.5

(Table 1 continues on next page)

TABLE 1: Estimated Accuracy (Area Under Receiver Operating Characteristic Curve), Sensitivity, Specificity, Positive Predictive Value (PPV), and Negative Predictive Value (NPV) of Dichotomized Variables and Some Combinations of These Variables for Detection of Hemiprostate Cancer (continued)

Combinations of Variables	Accuracy (%)[a]	Sensitivity (%)	Specificity (%)	PPV (%)	NPV (%)
All imaging models plus free-to-total PSA ratio (continued)					
T2WI plus DWI plus free-to-total PSA ratio	94.0 (0.200)	84.3	91.0	84.3	91.0
DWI plus DCE-MRI plus free-to-total PSA ratio	93.4 (0.090)	80.4	92.1	85.4	89.1
T2WI plus MRS plus free-to-total PSA ratio	93.5 (0.116)	84.3	92.1	86.0	91.1
MRS plus DCE-MRI plus free-to-total PSA ratio	93.1 (0.057)	80.4	92.1	85.4	89.1
T2WI plus DCE-MRI plus free-to-total PSA ratio	92.6 (0.050)	84.3	89.9	82.7	90.9
DWI plus free-to-total PSA ratio	92.0 (0.015)	70.6	96.6	92.3	85.1
MRS plus free-to-total PSA ratio	90.7 (0.003)	64.7	96.6	91.7	82.7
DCE-MRI plus free-to-total PSA ratio	90.2 (0.002)	70.6	93.3	85.7	84.7
T2WI plus free-to-total PSA ratio	90.8 (0.012)	76.5	92.1	84.8	87.2

Note—DCE-MRI = dynamic contrast-enhanced MRI, DWI = diffusion-weighted imaging, MRS = MR spectroscopy, PSA = prostate-specific antigen, T2WI = T2-weighted imaging.

[a]Numbers in parentheses are *p* values, for the individual significance level of the accuracy of each model versus the accuracy of the first model of its subgroup, without any correction for multiple comparisons.

The accuracy of the model combining all the imaging variables (T2WI, MRS, DWI, and DCE-MRI) (Fig. 1) in predicting prostate cancer was 87.3%, which was significantly higher than the diagnostic accuracy of each variable considered alone (DWI, 81.8%; MRS, 76.0%; DCE-MRI, 75.6%; and T2WI, 73.5%) and also higher than that for the combinations: 80.0% for T2WI plus DCE-MRI, 81.0% for MRS plus DCE-MRI, 81.4% for T2WI plus MRS, and 83.3% for T2WI, MRS, and DCE-MRI (Table 1). The accuracies of models MRS plus DWI (85.8%), T2WI plus DWI (84.8%), and DWI plus DCE-MRI (84.6%) have accuracy similar to that of the complete imaging model (87.3%) (Figs. 2 and 3). Moreover, all these models have the same sensitivity (72.5%), specificity (91.0%), PPV (82.2%), and NPV (85.3%). If we add free-to-total PSA ratio to the predictive imaging models, the accuracies increase significantly. The accuracy, sensitivity, specificity, PPV, and NPV of the complete model (T2WI, MRS, DWI, DCE-MRI, and free-to-total PSA ratio) were 95.2%, 88.2%, 89.9%, 83.3%, and 93.0%, respectively. The six models that combine free-to-total PSA ratio with only two imaging variables have accuracies ranging from 92.6% to 94.0%, not significantly lower than the complete model (Table 1) (Fig. 4). The sensitivities (80.4–84.3%), specificities (89.9–95.5%), PPVs (82.7–91.1%), and NPVs (89.1–91.1%) of these six models are not significantly different than those of the complete model. The highest accuracy from these six models is the combination of T2WI, DWI, and free-to-total PSA ratio (94.0%), showing sensitivity, specificity, PPV, and NPV of 84.3%, 91.0%, 84.3%, and 91.0%, respectively. In contrast, the accuracies of the four models that combine free-to-total PSA ratio with only one imaging variable are all significantly lower than that of the complete model (Table 1).

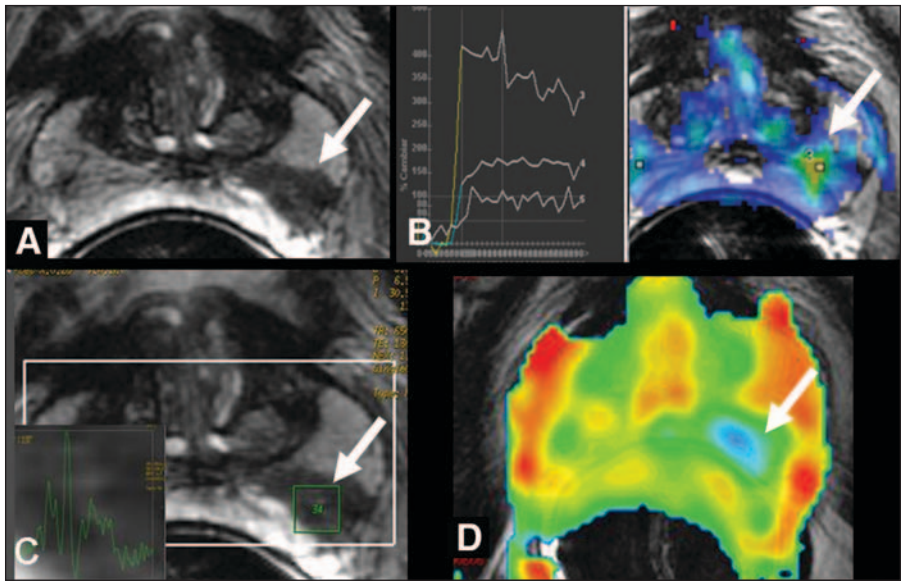

Fig. 2—60-year-old man with peripheral prostate cancer, with negative MR spectroscopy (MRS) imaging results and positive findings from T2-weighted imaging (T2WI), diffusion-weighted imaging (DWI), and dynamic contrast-enhanced (DCE) MRI images. Patient's prostate-specific antigen (PSA) level was 3.90 ng/mL, and his free-to-total PSA ratio was 7.5%.

A, Axial T2WI scan shows low-signal-intensity nodular lesion (*arrow*) within left peripheral zone, suspicious for cancer.

B, DCE-MRI images shows curve type 3 from region of interest of lesion (*arrow*) suspicious for cancer.

C, MRS image shows normal metabolic curve within voxel from lesion (*arrow*).

D, Apparent diffusion coefficient map from DWI shows restricted diffusion from lesion (*arrow*), suspicious for malignant tumor. Biopsy was positive for prostate cancer within peripheral zone.

Table 2 shows the sensitivity, specificity, PPV, and NPV on a per-patient basis for the models shown in Figure 4—T2WI, MRS, DWI, DCE-MRI, and free-to-total PSA ratio; T2WI, DWI, and free-to-total PSA ratio; T2WI, MRS, and DWI; T2WI plus DWI; and DWI alone—to realize the potential avoided biopsies.

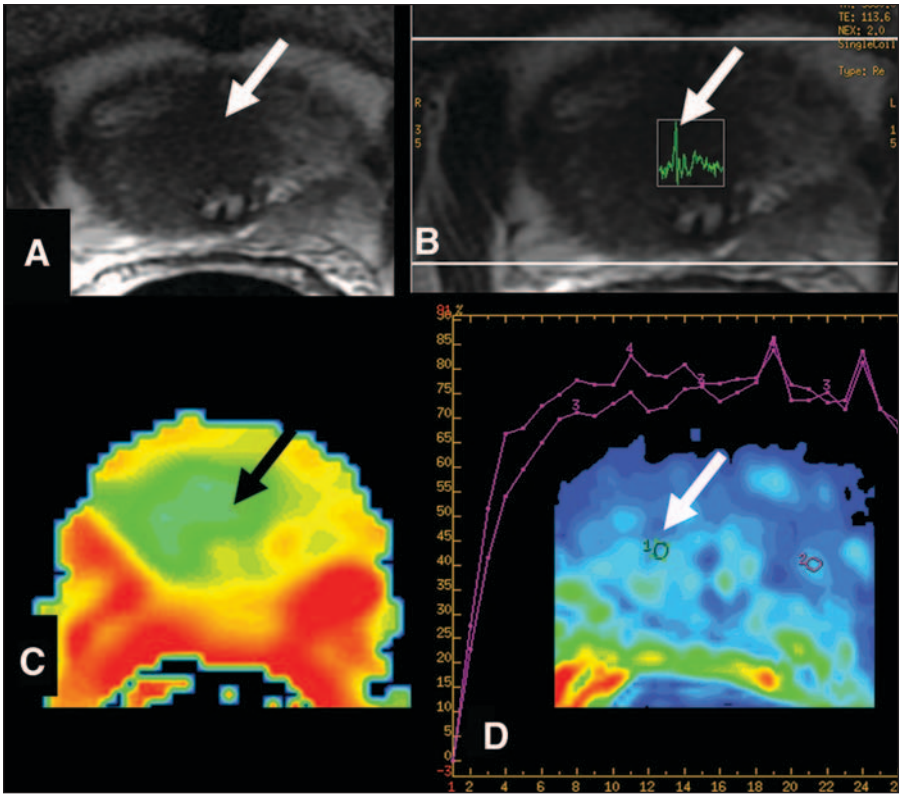

Fig. 3—64-year-old man with transitional prostate cancer, with negative dynamic contrast-enhanced (DCE) MRI findings and positive MRI results on T2-weighted imaging (T2WI), MR spectroscopy (MRS), and diffusion-weighted imaging (DWI). Patient's prostate-specific antigen (PSA) level was 7.90 ng/mL, and his free-to-total PSA ratio was 8.23%.
A, Axial T2WI scan shows low-signal-intensity nodular ill-defined lesion (*arrow*) within bilateral transitional zone suspicious for cancer.
B, MRS image shows pathologic metabolic curve within voxel from lesion, with high level of choline (*arrow*).
C, Apparent diffusion coefficient color map from DWI shows restricted diffusion from lesion, as low signal intensity (*arrow*), suspicious for malignant tumor.
D, DCE-MRI image on color-coded graph shows symmetric type 2 curve from region of interest of lesion (*arrow*) and within nontumoral tissue, considered nonsuspicious for cancer. Biopsy was positive for prostate cancer within transitional zone.

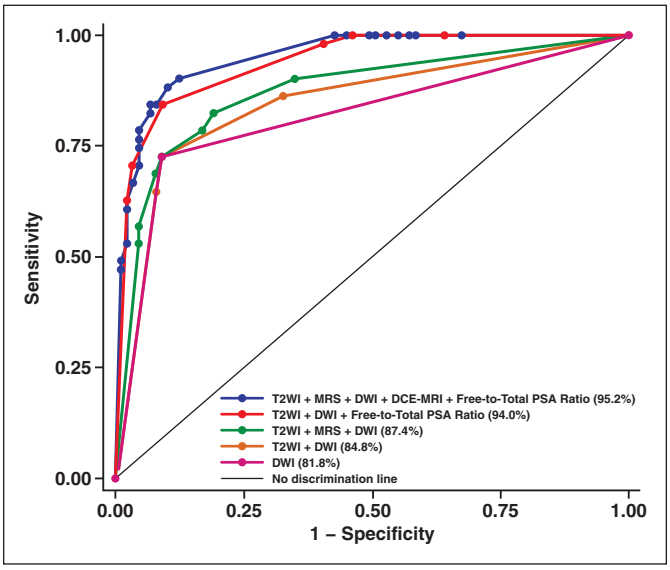

Fig. 4—Receiver operating characteristic (ROC) curves for different combinations of predictive variables: T2-weighted imaging (T2WI), MR spectroscopy (MRS), diffusion-weighted imaging (DWI), dynamic contrast-enhanced (DCE) MRI, and free-to-total prostate-specific antigen (PSA) ratio. Overall accuracy of each model given by area under corresponding ROC curves (in percentages) is shown in parentheses.

Discussion

We found that combining information from functional MRI with free-to-total PSA ratio improved the detection of prostate cancer before biopsy in patients with elevated PSA levels.

Previous studies have shown that adding data from one or two functional techniques (MRS, DWI, and DCE-MRI) improves prostate cancer detection [4–15, 25]. However, our results show that adding data from a third functional technique does not further improve detection; thus, not all the functional sequences need to be included in every MRI study. On the basis of these results, DWI should be one of the sequences included. In the only previous study to evaluate the value of including all three functional sequences, Riches et al. [26] also concluded that combining two functional parameters significantly improves prostate cancer detection over the use of any parameter alone and that adding a third parameter does not further improve detection. Despite the similarity of the results in these two studies, it is important to consider the different methods used. Both studies have the strength of separating the analysis from the peripheral and transitional zones; this is important because data from MRS, DWI, and DCE-MRI are not comparable between these two zones. However, unlike Riches et al., we excluded patients with recent biopsy results, thus eliminating possible interference in signal intensity from the previous procedure.

One of the significant results of our study is the benefit of combining clinical (free-to-total PSA ratio) and imaging data (MRI, MRS, DWI, and DCE-MRI) in early prostate cancer detection. We found that it could be useful to combine free-to-total PSA ratio with any functional imaging parameter, especially the combination of T2WI and DWI, in the workup for prostate cancer before indicating biopsy. Nevertheless, whenever we evaluate MRI sequences without clinical data, T2WI should be combined with some other functional sequences for prostate cancer detection, besides the DWI, MRS, or DCE-MRI technique.

Our results can help optimize MRI protocols and lower costs by making it unnecessary to include all the sequences in a prostate study. Because MRS is not widely available and also has the drawback of lacking a standardized evaluation method to ensure reproducibility [27], we suggest that the protocol for prostate cancer detection should include at least a DWI or DCE-MRI sequence or both. DWI has the advantages of being cheaper and easier to per-

TABLE 2: Estimated Sensitivity, Specificity, Positive Predictive Value (PPV), and Negative Predictive Value (NPV) on a Per-Patient Basis of Some Combinations of Dichotomized Variables for Detection of Prostate Cancer

Combinations of Variables	Sensitivity (%)	Specificity (%)	PPV (%)	NPV (%)
DWI	81.6 (31/38)	78.1 (25/32)	81.6 (31/38)	78.1 (25/32)
T2WI plus DWI	81.6 (31/38)	78.1 (25/32)	81.6 (31/38)	78.1 (25/32)
T2WI plus MRS plus DWI	78.9 (30/38)	81.3 (26/32)	83.3 (30/36)	76.5 (26/34)
T2WI plus DWI plus free-to-total PSA ratio	92.1 (35/38)	81.3 (26/32)	85.4 (35/41)	89.7 (26/29)
T2WI plus MRS plus DWI plus DCE-MRI plus free-to-total PSA ratio	94.7 (36/38)	81.3 (26/32)	85.7 (36/42)	92.9 (26/28)

Note—DCE-MRI = dynamic contrast-enhanced MRI, DWI = diffusion-weighted imaging, MRS = MR spectroscopy, PSA = prostate-specific antigen, T2WI = T2-weighted imaging.

form than DCE-MRI because it does not require the administration of exogenous contrast medium. Moreover, DWI was the most accurate of the imaging predictors when considered individually and it was also included in all the best models, with or without the combination of free-to-total PSA ratio. Although DWI has shown the better individual accuracy, it has high reported variability because of physiologic factors as well as technical factors that make it difficult to generally apply a certain ADC threshold for cancer detection [28–30].

We found moderate accuracy for each individual sequence, corroborating most previous reports about prostate cancer diagnosis with MRI [31–34]. For this reason, the MRI workup for prostate cancer detection should include a morphologic (T2WI) and a functional imaging technique. Whenever we consider the analysis for prostate cancer detection before biopsy using MRI sequences, at least two functional sequences could be used, because the use of a third functional technique does not further improve diagnostic cancer detection. Our study shows that combining free-to-total PSA ratio with data from T2WI, MRS, DWI, or DCE-MRI improves prostate cancer detection. Combining free-to-total PSA ratio with at least one functional imaging technique (MRS, DWI, or DCE-MRI) is more accurate than combining imaging variables without including free-to-total PSA ratio. Combining T2WI and a functional sequence could be adequate for cancer detection, especially if DWI is included.

In any case, the clinical approach to prostate cancer requires the gland to be considered as a whole unit. We suggest the following diagnostic algorithm: Patients with PSA level greater than 4.0 ng/mL and free-to-total PSA ratio less than 20% should undergo MRI, including functional sequences, to determine whether biopsy is necessary. Positive results at MRI call for TRUS biopsy (Fig. 5). Biopsying the target lesion detected at MRI would be more accurate than the current blind biopsy method, and the indication for biopsy would be more efficient than with current methods based on DRE and PSA values, because there is potential that, in the future, MRI data could be accurately transferred to TRUS images to help guide biopsy. Thus, performing prostate biopsy with functional MRI data available could improve the accuracy of biopsy results. For instance, if we choose the combination of T2WI plus DWI plus free-to-total PSA ratio to decide on a per-patient basis whether a biopsy should be performed, the model would have a sensitivity of 92.1%, specificity of 81.3%, PPV of 85.4%, and NPV of 89.7% and would save 41% (29 patients) of the biopsies (Table 2). Thus, the high NPV for the models where DWI and free-to-total PSA ratio are included could obviate a significant number of unnecessary biopsies.

Certain limitations and drawbacks of our study should be considered. One of the main limitations is the correlation of the imaging findings with the pathology findings: only 13 patients underwent prostatectomy, so the imaging-histologic correlation in the remaining 57 patients was based solely on the biopsy results. Given the low sensitivity of TRUS-guided biopsy [21], it is possible that some patients with negative biopsy results could have had cancer. The difficulty of correlating the MRI findings with biopsy results and even with surgical specimens is well known from attempts to ensure the correspondence of TRUS biopsy to suspicious areas on MRI [7]. Moreover, we should be aware of the more limited value of the study to analyze on a consensus reading instead of an independent reading method. Finally, larger studies are necessary to better assess these preliminary results.

In conclusion, our results show that a combination of free-to-total PSA ratio and multiparametric MRI can reliably detect the presence of prostate cancer on a per-patient basis. Therefore, in men with PSA levels greater than 4 ng/mL and free-to-total PSA ratios less than 20%, performing MRI has potential for avoiding a large number of negative biopsy results.

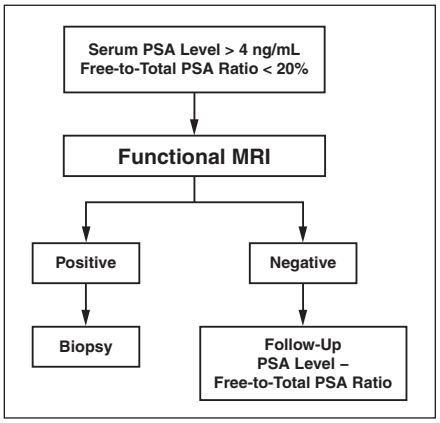

Fig. 5—Algorithm for early detection of prostate cancer based on morphologic and functional MRI and free-to-total prostate-specific antigen (PSA) ratio findings.

Acknowledgment

We thank John Giba for help with the English language.

References

1. Thompson IM, Pauler DK, Goodman PJ, et al. Prevalence of prostate cancer among men with a prostate-specific antigen level < or =4.0 ng per milliliter. *N Engl J Med* 2004; 350:2239–2246
2. Arcangeli CG, Ornstein DK, Keetch DW, Andriole GL. Prostate-specific antigen as a screening test for prostate cancer: The United States experience. *Urol Clin North Am* 1997; 24:299–306
3. Andriole GL, Catalona WJ. Using PSA to screen for prostate cancer: The Washington University experience. *Urol Clin North Am* 1993; 20:647–651
4. Cheikh AB, Girouin N, Colombel M, et al. Evaluation of T2-weighted and dynamic contrast-enhanced MRI in localizing prostate cancer before repeat biopsy. *Eur Radiol* 2009; 19:770–778
5. Mazaheri Y, Hricak H, Fine SW, et al. Prostate tumor volume measurement with combined T2-

weighted imaging and diffusion-weighted MR: correlation with pathologic tumor volume. *Radiology* 2009; 252:449–457

6. van Dorsten FA, van der Graaf M, Engelbrecht MR, et al. Combined quantitative dynamic contrast-enhanced MR imaging and ^{1}H MR spectroscopic imaging of human prostate cancer. *J Magn Reson Imaging* 2004; 20:279–287
7. Futterer JJ, Heijmink SW, Scheenen TW, et al. Prostate cancer localization with dynamic contrast-enhanced MR imaging and proton MR spectroscopic imaging. *Radiology* 2006; 241:449–458
8. Reinsberg SA, Payne GS, Riches SF, et al. Combined use of diffusion-weighted MRI and ^{1}H MR spectroscopy to increase accuracy in prostate cancer detection. *AJR* 2007; 188:91–98
9. Mazaheri Y, Shukla-Dave A, Hricak H, et al. Prostate cancer: identification with combined diffusion-weighted MR imaging and 3D ^{1}H MR spectroscopic imaging—correlation with pathologic findings. *Radiology* 2008; 246:480–488
10. Haider MA, van der Kwast TH, Tanguay J, et al. Combined T2-weighted and diffusion-weighted MRI for localization of prostate cancer. *AJR* 2007; 189:323–328
11. Langer DL, van der Kwast TH, Evans AJ, Trachtenberg J, Wilson BC, Haider MA. Prostate cancer detection with multi-parametric MRI: logistic regression analysis of quantitative T2, diffusion-weighted imaging, and dynamic contrast-enhanced MRI. *J Magn Reson Imaging* 2009; 30: 327–334
12. Kozlowski P, Chang SD, Jones EC, Berean KW, Chen H, Goldenberg SL. Combined diffusion-weighted and dynamic contrast-enhanced MRI for prostate cancer diagnosis: correlation with biopsy and histopathology. *J Magn Reson Imaging* 2006; 24:108–113
13. Kumar V, Jagannathan NR, Kumar R, et al. Correlation between metabolite ratios and ADC values of prostate in men with increased PSA level. *Magn Reson Imaging* 2006; 24:541–548
14. Noworolski SM, Vigneron DB, Chen AP, Kurhanewicz J. Dynamic contrast-enhanced MRI and MR diffusion imaging to distinguish between glandular and stromal prostatic tissues. *Magn Reson Imaging* 2008; 26:1071–1080
15. Chen M, Dang HD, Wang JY, et al. Prostate cancer detection: comparison of T2-weighted imaging, diffusion-weighted imaging, proton magnetic resonance spectroscopic imaging, and the three techniques combined. *Acta Radiol* 2008; 49:602–610
16. Kubota Y, Kamei S, Nakano M, Ehara H, Deguchi T, Tanaka O. The potential role of prebiopsy magnetic resonance imaging combined with prostate-specific antigen density in the detection of prostate cancer. *Int J Urol* 2008; 15:322–326
17. Vilanova JC, Comet J, Barceló-Vidal C, et al. Peripheral zone prostate cancer in patients with elevated PSA levels and low free-to-total PSA ratio: detection with MR imaging and MR spectroscopy. *Radiology* 2009; 253:135–143
18. Akin O, Sala E, Moskowitz CS, et al. Transition zone prostate cancers: features, detection, localization, and staging at endorectal MR imaging. *Radiology* 2006; 239:784–792
19. Kurhanewicz J, Vigneron DB, Hricak H, Narayan P, Carroll P, Nelson SJ. Three-dimensional H-1 MR spectroscopic imaging of the in situ human prostate with high (0.24-0.7-cm^{3}) spatial resolution. *Radiology* 1996; 198:795–805
20. Ren J, Huan Y, Wang H, et al. Dynamic contrast-enhanced MRI of benign prostatic hyperplasia and prostatic carcinoma: correlation with angiogenesis. *Clin Radiol* 2008; 63:153–159
21. Wefer AE, Hricak H, Vigneron DB, et al. Sextant localization of prostate cancer: comparison of sextant biopsy, magnetic resonance imaging and magnetic resonance spectroscopic imaging with step section histology. *J Urol* 2000; 164:400–404
22. Okamura K, Takaba H, Kamihira O, et al. Determination of the relative probability for prostate cancer to avoid unnecessary biopsy. *Int J Urol* 2005; 12:346–352
23. DeLong ER, DeLong DM, Clarke-Pearson DL. Comparing the areas under two or more correlated receiver operating characteristic curves: a nonparametric approach. *Biometrics* 1988; 44:837–845
24. Leisenring W, Alonzo T, Pepe MS. Comparisons of predictive values of binary medical diagnostic tests for paired designs. *Biometrics* 2000; 56: 345–351
25. Kozlowski P, Chang SD, Meng R, et al. Combined prostate diffusion tensor imaging and dynamic contrast enhanced MRI at 3T: quantitative correlation with biopsy. *Magn Reson Imaging* 2010; 28:621–628
26. Riches SF, Payne GS, Morgan VA, et al. MRI in the detection of prostate cancer: combined apparent diffusion coefficient, metabolite ratio, and vascular parameters. *AJR* 2009; 193:1583–1591
27. Kurhanewicz J, Vigneron DB. Advances in MR spectroscopy of the prostate. *Magn Reson Imaging Clin N Am* 2008; 16:697–710
28. Wang XZ, Wang B, Gao ZQ, et al. Diffusion-weighted imaging of prostate cancer: correlation between apparent diffusion coefficient values and tumor proliferation. *J Magn Reson Imaging* 2009; 29:1360–1366
29. Sato C, Naganawa S, Nakamura T, et al. Differentiation of noncancerous tissue and cancer lesions by apparent diffusion coefficient values in transition and peripheral zones of the prostate. *J Magn Reson Imaging* 2005; 21:258–262
30. Hosseinzadeh K, Schwarz SD. Endorectal diffusion-weighted imaging in prostate cancer to differentiate malignant and benign peripheral zone tissue. *J Magn Reson Imaging* 2004; 20:654–661
31. Vilanova JC, Comet J, Capdevila A, et al. The value of endorectal MR imaging to predict positive biopsies in clinically intermediate-risk prostate cancer patients. *Eur Radiol* 2001; 11:229–235
32. Scheidler J, Hricak H, Vigneron DB, et al. Prostate cancer: localization with three-dimensional proton MR spectroscopic imaging—clinicopathologic study. *Radiology* 1999; 213:473–480
33. Engelbrecht MR, Huisman HJ, Laheij RJ, et al. Discrimination of prostate cancer from normal peripheral zone and central gland tissue by using dynamic contrast-enhanced MR imaging. *Radiology* 2003; 229:248–254
34. desouza NM, Reinsberg SA, Scurr ED, Brewster JM, Payne GS. Magnetic resonance imaging in prostate cancer: the value of apparent diffusion coefficients for identifying malignant nodules. *Br J Radiol* 2007; 80:90–95